41 TEMPERATURE FIELD AND CONCRETE STRESSES IN A FOUNDATION PLATE

P. PAULINI and D. BILEWICZ
Institut für Baustofflehre and Materialprüfung, Universität Innsbruck, Innsbruck, Austria

Abstract
Hydration temperatures can cause dividing cracks in thickwalled concrete building members. The temperature field in a foundation plate was measured in the first week of concrete hardening. Hydration temperatures are clearly influenced by day-night changes of air temperatures. Calculations of concrete stresses showed that external restraint stresses principally are responsible for thermal cracking. These can been reduced with slide sheets to the extent that the occurrence of dividing cracks can be avoided.
Keywords: Cracking, Heat of Hydration, Restraint Stresses, Structural Members (Foundation Plate), Temperature Fields

1 Introduction

Concrete temperature stresses resulting from hydration heat are significant for thick-walled watertight building members such as foundation plates and walls or tunnel linings in ground water. In such building components thermal stresses can lead to cracks in early age concrete and put at risk the component's performance. Reinforcement cannot prevent the occurrence of cracks, it can only limit crack widths and crack distribution. The aim of the engineer is therefore to avoid temperature stresses to a large extent by e.g. the following methods

- reduction of fresh concrete temperature
- active cooling of the building component during hardening time
- reduction of cement content or use of low heat cement
- reduction of restraint.

The cement type as the source of hydration temperatures has an important influence on the cracking behaviour. Springenschmid (1991,1992) shows that concretes with the same cement type but from different producers may have considerable differences in their cracking temperatures. The lowest tendency to cracking was found in cements with a low hydration temperature rise and low alkali content. This varying reaction behaviour of cements in the early phase was also pointed out by Paulini (1992). In national standards no specifications exist for achievable hydration levels for the early cement reaction. Requirements of high demould strength (e.g. for tunnel lining concrete 5 MPa after 12 hrs) often conflict with a low hydration temperature rise. Site

Thermal Cracking in Concrete at Early Ages. Edited by R. Springenschmid. Published 1994 by E & FN Spon, 2–6 Boundary Row, London SE1 8HN, UK. ISBN: 0 419 18710 3.

management often has to conduct its own trials to choose a suitable cement type. Slide sheets are therefore increasingly being used, where it is statically possible, to avoid thermal cracking of building members, Simons (1988), Schade (1989).

2 Building site and laboratory trials

During concreting work for the extension of the Innsbruck sewerage plant an SRPC cement and slide sheets were used to avoid thermal cracking in a foundation plate. The plate was a 55 cm thick, 10 by 10 m, reinforced, watertight foundation plate. The concrete used was a B300 K3 GK22 WU according to the Austrian standard ÖN B 4200/T10. The following mix design was used:

Cement PZ 375 HS (SRPC)	340 kg/m^3
Water	156 kg/m^3
Aggregates 0/22 mm	1952 kg/m^3
Plasticiser BV1	2.04 kg/m^3

In a field measurement programme concrete temperatures were to be recorded for the first week of hardening. The measurement were made in summer 1993 in a period in which day-night temperatures fluctuated considerably. Hydration temperatures were measured by means of NiCr-Ni thermocouples (TC). A thermistor signal served as the reference temperature. Five TC's were placed in the concrete plate symmetrically to the neutral axis. In addition the air temperature was recorded 5 cm above the surface. The TC's were placed in a plastic tube, which was then filled with PU foam. The completed sensor was fixed to the reinforcement mesh and connected to a data logger. Fig.1 shows a diagram of the sensor.

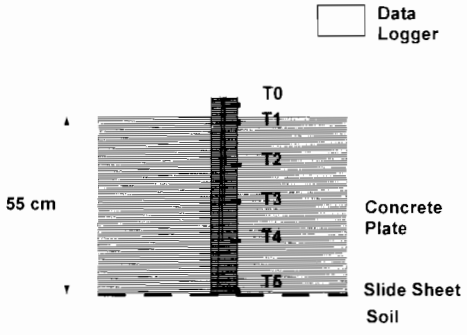

Fig. 1. Thermocouple sensor unit

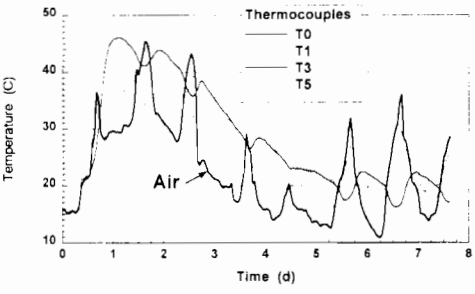

Fig. 2. Air and concrete temperature readings

Fig. 2 shows the recorded air temperature T0, concrete temperature T1 at the surface, T5 at the bottom and the plate mid temperature T3. The time scale was chosen in such a way that day numbers refer to midnight. Concrete work took place from 7.00-10.30 a.m. with a fresh temperature of 21 °C. Approximately 5 hours after casting the hydration gain starts with a maximum temperature increase of 25 °C. 18 hours after casting the maximum core temperature of 46 °C is reached and the cooling period is initiated. The air temperature T0 is clearly influenced by the

hydration peak. Air temperature changes of 15 - 20 °C between day and night were observed. On the 4th and 5th day air temperature fell suddenly, then increased again up to the 8th day. The air temperature cycles propagate into the concrete plate (Fig.3). During short daytime temperature peaks, heat is transferred to the plate while during the night the gradient is reversed and heat dissipates from the plate. The temperature wave reaches the bottom only after 8-10 hrs. Daily temperature gain on the surface thus partly coincides with temperature loss at the bottom. This explaines the oscillating stresses in the plate calculated subsequently.

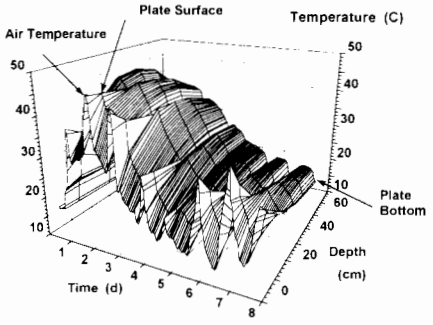

Fig. 3. Concrete temperature field

Age (h)	Compr. Strength (MPa)	Flexural Strength (MPa)	Splitting Strength (Mpa)	E-Mod. (GPa)
24	19.6	3.75	1.99	28.0
33	20.8	3.82	1.92	29.9
49	24.7	3.15	2.26	34.1
96	25.2	3.35	2.59	32.0

Tab. 1. Concrete properties

Development of concrete strength and elastic modulus were measured for the first four days. Concrete prisms (12/12/36 cm) were stored from 6 hours onwards in a climatic cabinet at constant 30 °C and 90% r.h. The measured values are shown in table 1.

3 Temperature stresses

Temperature stresses in building members consist of three different fractions which are shown in Fig. 4. Internal stresses σ_i arise from nonlinear temperature distribution over the cross section and are calculated so as to not give rise to any normal force and moment in the cross section. External restraint stresses arise only when temperature deformations of the building member are prevented. Warping stresses σ_w result from a linear temperature distribution between opposite surfaces while restraint normal stresses σ_n arise from uniform temperature differences relative to a stress free reference state T_0. This means for the stress state of Fig. 4 that the whole cross section is subjected to a deformation restraint. In practice such conditions seldom exist. Generally there is only a friction restraint in the border plane to soil or to the adjacent component, while the opposite surface remains free of restraint.

The further calculation is based on the principle shown in Fig.5. Here an eccentric friction force F_c acts on the plate bottom and produces a stress state σ_f. The friction force F_c can be determined by requiring that thermal deformations of the unrestrained plate and elastic deformations resulting from friction force on the bottom side must vanish. The assumption of a linear elastic stress-strain behaviour for concrete is true

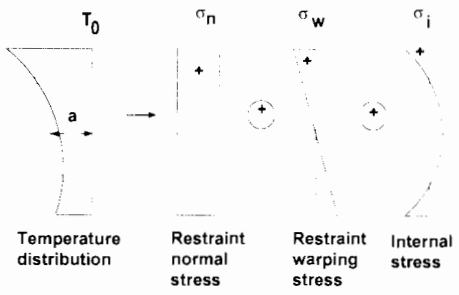

Fig. 4. Thermal stress fractions with a centric restraint

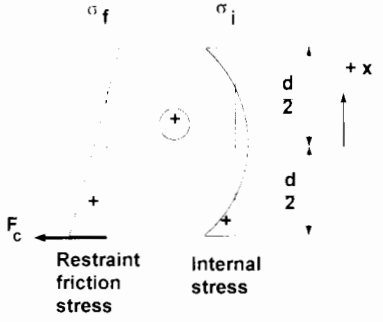

Fig. 5. Thermal stress fractions with an eccentric restaint

for small compression stresses and also for tension stresses. Heilmann et al (1969), Reinhardt (1984). Relaxation of early age concrete is taken into account according to Rostásy and Henning (1990) by introducing a relaxation factor k_r and a reduced elastic modulus E_r. The reference temperature T_0 for a state without any stress was found to be some degrees lower than the maximum hydration temperature, Springenschmid (1991). For simplicity in this calculation T_0 is considered as maximum hydration temperature (max a_j Eq. 9) and restraint stresses are related to this state.

3.1 Internal stresses

Internal stresses arise from a nonlinear temperature distribution. First we describe the temperature distribution T(x) in the plate as a polynome of coordinate x (Eq.1). The origin of x is set in the neutral axis of the plate (Fig. 5).

$$T(x) = \sum_{i=0}^{n} C_i \cdot x^i \qquad (1)$$

Coefficients C_i are determined in such a way that the measured temperatures Tm in the support points s_i are matched exactly by the polynom. The five TC positions s_i, i=0..4, were arranged symmetrically to the neutral axis at 0, ±100 and ±260 mm defining a temperature polynom T(x) of 4th degree. With the inverse of the polynom matrix M (Eq.2) coefficients C_j for each hourly measurement time j=1..183 can be calculated (Eq. 3).

$$M_i = s^i \qquad (2)$$

$$C_j = M^{-1} \cdot Tm_j \qquad (3)$$

The polynom T(x) represents the temperature field for each depth in the plate and each of the measured times j. Now we look for a linear temperature distribution G(x) whereby stresses from the temperature difference T(x)-G(x) do not result in normal forces or moments in the plate. We assume the cross section to be a rectangle of depth d.

$$G_j(x) = a_j + b_j \cdot x \tag{4}$$

First we find the integrals of temperature TI and temperature moments TM over the plate depth d (Eq.5,6).

$$TI_j = \int_{-d/2}^{d/2} T(x)_j \cdot dx \tag{5}$$

$$TM_j = \int_{-d/2}^{d/2} T(x)_j \cdot x \cdot dx \tag{6}$$

The same values for the linear temperature distribution G(x) become (Eq. 7,8)

$$GI_j = a_j \cdot d \tag{7}$$

$$GM_j = b_j \cdot \frac{d^3}{12} \tag{8}$$

The coefficients a and b of the linear temperature distribution G(x) are calculated by equalizing both the temperature and the temperature moment integrals (Eq.9,10)

$$a_j = \frac{1}{d} \cdot \int_{-d/2}^{d/2} T(x)_j \cdot dx \tag{9}$$

$$b_j = \frac{12}{d^3} \cdot \int_{-d/2}^{d/2} T(x)_j \cdot x \cdot dx \tag{10}$$

Coefficient a represents the average temperature and coefficient b the slope of the linear distribution G(x). Fig. 6 is a plot of the coefficients over time, while Fig. 7 gives temperature distributions T(x) and G(x) over depth as well as the measured temperatures Tm at 38 hours after casting.

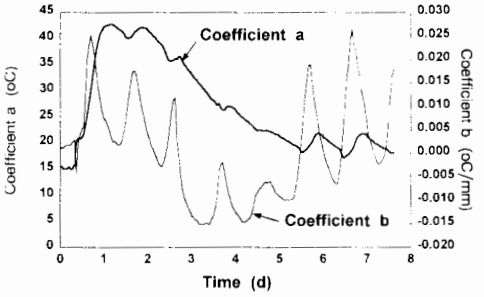

Fig. 6. Coefficients of linear temperatur distribution G(x)

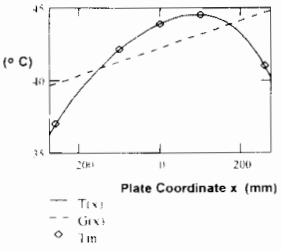

Fig. 7. Calculated and measured plate temperature distribution

Internal stresses σ_i are found with Eq. 11 from the difference of both temperature distributions T and G.

$$\sigma_i(x)_j = (T(x) - G(x))_j \cdot E_r \cdot \alpha_t \tag{11}$$

$$E_r = k_r \cdot E \tag{12}$$

E_r is a reduced elastic modulus of concrete according to Eq. 12. The relaxation factor k_r for an effective concrete age of 2-3 days is given as 0.65 and for more then

5 days as 0.85 , Rostásy and Henning (1990) . In this calculation k_r was set at an average value of 0.75. The elastic modulus was assumed at 32 GPa (Tab. 1) and the coefficient of thermal deformation α_t at 9.10^{-6}. Fig. 8 represents calculated internal stresses which are clearly influenced by daily air temperature changes.

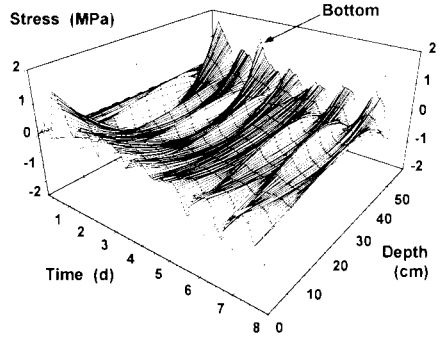

Fig. 8. Internal stress field

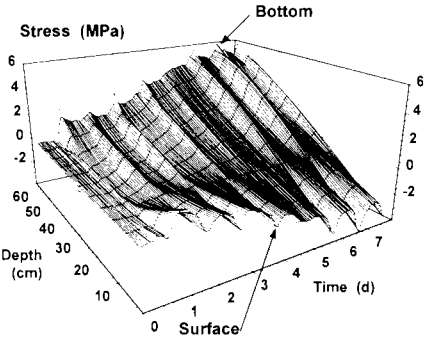

Fig. 9. Thermal stress field, combind internal and external restraint stresses

3.2 External restraint stresses

External restraint stresses in the plate arise only from the effect of friction forces F_c (Fig. 5). By requiring that elastic and thermic deformations in the restraint plane must vanish, we get for a rectangular section the friction force F_c at time j to

$$F_{c,j} = [(T_0 - a_j) + b_j \cdot x] \, f \, E_r \, \alpha_t \, \frac{d}{4} \tag{13}$$

The coefficient f $(0 \leq f \leq 1)$ is introduced to take into account the effect of the slide sheet and is set at 1.0 for a rigid support. In Fig. 10 the rise in the friction force F_c is shown from the point of reaching zero stress temperature T_0 (max a_j) onwards. Again the influence of air temperature cycles is apparent. External restraint stresses σ_f were calculated using Eq. 14 and are summarised with the internal stresses in Fig. 9.

$$\sigma_f = \frac{F_c}{d} \left(1 - \frac{6}{d} x \right) \tag{14}$$

In Fig. 11 plate edge stresses and stresses in the neutral axis are represented together with measured flexural strength $f_{c,fl}$ and uniaxial tensile strength $f_{c,t}$. Tensile strength $f_{c,t}$ was not measured and set for comparison at $f_{c,fl}$ / 2 according EC2. Concrete strengths were measured for the first four days (Tab. 1) and were subsequently drawn constant. Restraint stresses exceed internal edge stresses from approximately the second day on and act mainly as a bending load on the plate. The criterion for the occurrence of a dividing crack through the whole plate is the attainment of uniaxial concrete tension strength $f_{c,t}$ in the neutral axis of the plate. This occurs for a short time on the 6th and 7th day in the early afternoon. While cracks on the bottom side can propagate once flexural strength $f_{c,fl}$ is exceeded on the

4th day, they do not occur on the surface because of flexural compression stresses.

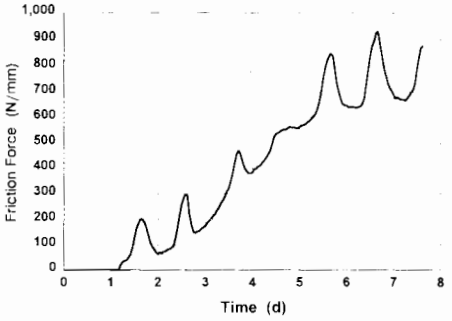

Fig. 10. Eccentric restraint friction force F_c , f=1

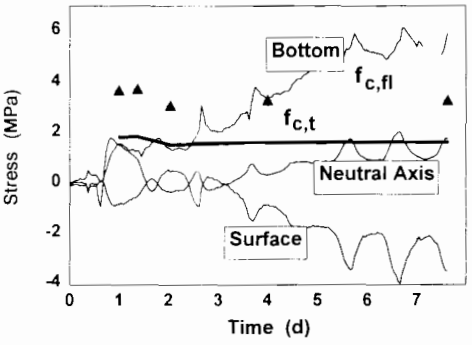

Fig.11. Concrete stresses and strength, f=1

3.3 Effect of slide sheets

Slide sheets are being used increasingly to ensure the avoidance of cracks in thick-walled and long concrete members, Simons (1988), Schade (1989). They reduce external restraint stress which in our case make up appr. 70% of total thermal stress. Bitumen sheeting has proven particularly effective because hydration temperatures improve its viscous deformation behaviour.

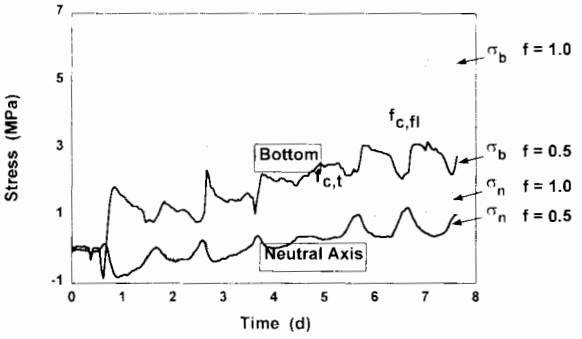

Fig. 12. Concrete stresses with varying slide sheet influence f, n = plate neutral axis, b = plate bottom

In the previous calculation the coefficient f was set at 1.0 assuming a rigid support. This value will mainly be influenced by the support conditions and the elasticity of soil. At the moment an exact estimation of external restraint stress reduction of slide sheets is not possible because suitable trials have yet to be carried out. Assuming a reduction of 50% (f=0.50), plate edge stress becomes lower than concrete flexural strength and neutral axis stress lower then uniaxial tensile strength. Fig. 12 shows this comparison between stresses in the plate bottom (σ_b) and the neutral axis (σ_n) for f=1.0 and f=0.50. However, in the foundation plate we studied, no dividing cracks actually occured.

4 Conclusion

Concrete cracks in thickwalled building members can be induced by hydration temperatures particularly where temperature deformations are restricted. This can be caused by friction in a plane between the building member and the soil or the adjacent building component. In many such cases the use of low heat cements and slide sheets prevents thermal cracking.

A method of calculating thermal concrete stresses based on temperature profile measurements has been presented. The calculation has been applied on hydration temperatures of a foundation plate. The temperature distribution was measured in a 55 cm thick foundation slab during the first week of concrete hardening. Maximum core temperature gain was 25 °C and was reached 18 hours after casting. It was found, that daily air temperature changes influence considerably concrete temperatures and stresses. The night cooling period particularly propagates into the concrete and reaches the plate bottom after a time lag of 8-10 hours. Concrete stresses were calculated from the temperature field assuming linear elastic material behaviour. With rigid support conditions, oscillating stresses should lead to dividing cracks 6 to 7 days after concrete casting. Thermal dividing cracks were avoided using slide sheets between foundation plate and soil. The degree of stress reduction of slide sheets is not yet completely understood. Further experiments will clarify this influence.

The method can be applied to building members which have a friction restraint on one surface like foundation slabs and walls, tunnel linings or watertight building members in contact with soil. The application to free walls on foundations has not been proved but should be possible in principle.

References

Heilmann H., Hilsdorf H., Finsterwalder K.: (1969), *Festigkeit und Verformung von Beton unter Zugspannung*, DAfStb. H.203, Ernst & Sohn, Berlin

Paulini P.: (1992), *A weighing method for cement hydration*. Proc. 9th ICCC., New Delhi, Vol.IV. pp.248-254

Reinhardt H.W.: (1984),*Verhalten des Betons im verformungsgesteuerten axialen Zugversuch*. Fortschritte im konstruktiven Ingenieurbau, Rehm-Festschrift, Ernst & Sohn, Berlin, pp.221-227

Rostásy F.S., Henning W.: *(1984), Zwang und Rißbildung in Wänden auf Fundamenten*. DAfStb. H.407, Beuth Verlag, Berlin

Schade D.: (1989), *Tiefgarage der Kongreßhalle Böblingen - eine weiße Wanne 10 m tief im Grundwasser*. Bautechnik, 66, pp.217-219

Simons H.J.: (1988), *Konstruktive Gesichtspunkte beim Entwurf weißer Wannen*. Bauingenieur, 63, pp.429-437

Springenschmid R.: (1991), *Risse im Beton infolge Hydratationswärme*. Zement-Kalk-Gips, 44.Jg., H.3, pp.132-138

Springenschmid R. Breitenbücher R.: (1992), *Influence of cement on thermal cracking of concrete at early ages*. Proc. 9th ICCC., New Delhi, Vol.V, pp.122-128